International Journal of Mass Spectrometry 179/180 (1998) 43–54

Sulfur–sulfur three-electron bond dissociation enthalpies of dialkyl sulfide dimer radical cations

Sam P. de Visser[a,1], F. Matthias Bickelhaupt[b], Leo J. de Koning[a], Nico M.M. Nibbering[a,]*

[a]*Institute of Mass Spectrometry, University of Amsterdam, Nieuwe Achtergracht 129, NL-1018 WS Amsterdam, The Netherlands*
[b]*Fachbereich Chemie, Philipps-Universität Marburg, Hans-Meerwein-Straße, D-35032 Marburg, Germany*

Received 7 February; accepted 22 June 1998

Abstract

We have prepared the dimer radical cations $(R_2S)_2^{+\cdot}$ of a series of dialkyl sulfides R_2S (= Me_2S, MeEtS, Et_2S, Et-*n*-PrS, *n*-Pr_2S, *i*-Pr_2S, *n*-Bu_2S) in an FT-ICR cell. These have been found to react with neutral dialkyl sulfides by ligand exchange. By studying the $(R_2S)_2^{+\cdot} + 2Et_2S \rightleftarrows (Et_2S)_2^{+\cdot} + 2\ R_2S$ equilibria the associated Gibbs energy changes ΔG^0 have been determined. From these, the sulfur–sulfur bond dissociation enthalpies (BDE) of the dimers could be estimated using the relationship $\mathrm{BDE}[(R_2S)_2^{+\cdot}] = -\Delta G^0 - T\Delta S^0 + \mathrm{IE}[Et_2S] - \mathrm{IE}[R_2S] + \mathrm{BDE}[Et_2S)_2^{+\cdot}]$ and taking literature values for $\mathrm{BDE}[(Et_2S)_2^{+\cdot}]$ and the ionization energies $\mathrm{IE}[R_2S]$. The entropies of reaction ΔS^0 have been estimated using statistical thermodynamics and computationally optimized structures. The 298 K sulfur–sulfur BDE values thus obtained are 115, 112, 115, 107, 103, and 97 kJ mol^{-1} for $(Me_2S)_2^{+\cdot}$, $(MeEtS)_2^{+\cdot}$, $(Et_2S)_2^{+\cdot}$, $(Et\text{-}n\text{-}PrS)_2^{+\cdot}$, $(n\text{-}Pr_2S)_2^{+\cdot}$ and $(n\text{-}Bu_2S)_2^{+\cdot}$, respectively. The trend in S–S bond strength as well as the various contributions to ΔS^0 are discussed. (Int J Mass Spectrom 179/180 (1998) 43–54) © 1998 Elsevier Science B.V.

Keywords: Sulfur–sulfur bond energies; Disulfide radical cations; FT-ICR equilibria measurements; Theoretical calculations; Steric effects

---

1. Introduction

One of the strongest intermolecular bonds in dimer radical cations is the two-center three-electron (2c3e) bond. In the gas phase, this type of bond has been observed for dimer radical cations of dialkyl sulfides, $(R_2S)_2^{+\cdot}$ (**1**) [1–7], and alkyl halides, $(RX)_2^{+\cdot}$ (**2**) [8,9]. The dissociation energy of the 2c3e bond in these species varies from ca 90 to 120 kJ mol^{-1}. This is significantly higher than, for instance, the bond strength of 81 ± 5 kJ mol^{-1} of the water dimer radical cation [10]. The relatively high strengths observed for S ∴ S and X ∴ X 2c3e bonds may be regarded as resulting from a covalent bond with formal bond order of 1/2.

$$\underset{\mathbf{1}}{R_2S \therefore SR_2^{+\cdot}} \qquad \underset{\mathbf{2}}{RX \therefore XR^{+\cdot}}$$

It is indispensable for a profound understanding of the S ∴ S 2c3e bond to have reliable experimental data at one's disposal. Therefore, in the present study, we have determined the sulfur–sulfur bond dissocia-

---

* Corresponding author.

[1] Present address: Department of Theoretical Chemistry, King's College London, Strand WC2R 2LS, London, UK.

Dedicated to Professor Fulvio Cacace for his many contributions to gas-phase ion chemistry.

1387-3806/98/$19.00 © 1998 Elsevier Science B.V. All rights reserved
PII S1387-3806(98)14072-1

tion enthalpies (BDE) of a series of dialkyl sulfide dimer radical cations $(R_2S)_2^{+\cdot}$ through a combined FT-ICR mass spectrometric and theoretical approach. By studying ligand exchange equilibria of the type of Eq. (1) in the cell of an FT-ICR mass spectrometer, the corresponding equilibrium constants, K, and Gibbs reaction energies, ΔG^0, have been experimentally determined:

$$(R_2S)_2^{+\cdot} + 2Et_2S \rightleftarrows (Et_2S)_2^{+\cdot} + 2R_2S \qquad (1)$$

The ΔG^0 values were then converted to enthalpies by calculating or estimating the associated reaction entropies ΔS^0 using statistical thermodynamics and, amongst others, ab initio theory. Equilibrium studies are well known for the determination of thermochemical properties of compounds [11]. The bond dissociation enthalpies from our present, more accurate equilibrium study are compared with those obtained previously using CID threshold experiments [7]. The trend in S–S bond strength along our series of dialkyl sulfide dimer radical cations is discussed in terms of steric repulsion versus electronic effects on the 2c3e bond. Furthermore, the reaction entropies ΔS^0 of equilibrium 1 are resolved into their translational, rotational, and vibrational components.

2. Experimental

2.1. FT-ICR experiments

The experiments were performed with a Bruker CMS-47X Fourier transform ion cyclotron resonance (FT-ICR) mass spectrometer [12,13], equipped with an external electron ionization (EI) source and a 4.7 T superconducting magnet.

In the EI source the dialkyl sulfide molecules were ionized using 20 eV electrons. Subsequently, the ions were transferred to the cell, where dialkyl sulfide was present. In the FT-ICR cell, the dialkyl sulfide dimer radical cations were produced by association of the dialkyl sulfide radical cations with the dialkyl sulfides. In reaction 2, A represents a dialkyl sulfide with two saturated alkyl groups:

$$A^{+\cdot} + A \rightarrow A_2^{+\cdot} \qquad (2)$$

In the FT-ICR cell the pressure of the individual components was kept between 10^{-8} and 10^{-7} mbar (ion gauge manometer reading) with a background pressure of less than 10^{-9} mbar, while in the EI source the pressure of the compounds was between 10^{-4} and 10^{-3} mbar.

The ion beam was gated for 40 ms and subsequently a collision gas, either nitrogen or argon, was added into the cell through a pulsed valve system, in order to thermalize the dimer radical cations [10]. The pulsed valve was gated four times for 120 ms each time followed by a delay time of 3 s. The dimer radical cations then were isolated in the cell. The reactivity of the dimer radical cations was studied toward various dialkyl sulfides with different saturated alkyl groups.

If possible, equilibrium studies were performed between two radical cation dimers of two different dialkyl sulfides A and B, reaction 3.

$$A_2^{+\cdot} + 2B \rightleftarrows 2A + B_2^{+\cdot} \qquad (3)$$

The equilibrium constant (K) for reaction 3 can be described with Eq. (4).

$$K = \frac{I_{B_2^{+\cdot}}\, p_A^2}{I_{A_2^{+\cdot}}\, p_B^2} \qquad (4)$$

The equilibrium abundance ratios $I(B_2^{+\cdot})/I(A_2^{+\cdot})$ were accurately determined from the mass spectra of the reaction mixtures and the equilibrium partial pressure ratios p_A/p_B were obtained from the ion gauge manometer readings corrected for the sensitivity for the gases X, using the relationship $R_X = 0.36\alpha + 0.30$ of Bartmess and Georgiadis [14] with polarizabilities α from Miller [15]. The sum of the partial pressures was below 10^{-7} mbar. The equilibrium constant was converted into the Gibbs free energy difference (ΔG^0), using Eq. (5):

$$\Delta G^0 = -RT \ln K \qquad (5)$$

In formula (5), R is the gas constant (8.314 J mol^{-1} K^{-1}) and T the absolute temperature, which is estimated to be 298 K.

2.2. Materials

All chemicals employed here were commercially available and used without further purification.

2.3. Computational procedures

Calculations were performed on an RS/6000 workstation using the GAUSSIAN 94 program packages [16]. Geometry optimizations were performed at different levels of theory, see Results section. In the case of radical cations the applicability of both the restricted open-shell Hartree Fock (ROHF) procedure as well as the unrestricted Hartree Fock (UHF) procedure have been tested. Frequency calculations were performed at the HF/6-31G(d) level of theory with geometry optimized structures at this level.

Furthermore, we report the preliminary results of density-functional theoretical (DFT) computations, which were carried out with the Amsterdam Density Functional (ADF) program, using the local density approximation (LDA) as well as nonlocal corrections (BP86 level) together with STO basis sets of TZ2P quality for sulfur and DZP for carbon and hydrogen, see [17] for details.

3. Results and discussion

3.1. Preparation of dialkylsulfide dimer radical cations

Using association reactions [reaction (2)] of an alkyl sulfide radical cation with an alkyl sulfide, the dimer radical cations of methanethiol, dimethyl sulfide (Me_2S), methyl ethyl sulfide (MeEtS), diethyl sulfide (Et_2S), ethyl-*n*-propyl sulfide (Et-*n*-PrS), di-*n*-propyl sulfide (*n*-Pr_2S), di-*i*-propyl sulfide (*i*-Pr_2S), di-*n*-butyl sulfide (*n*-Bu_2S) and di-*t*-butyl sulfide (*t*-Bu_2S) were generated.

In general, every dialkyl sulfide dimer radical cation, with the exception of $(t\text{-}Bu_2S)_2^{+\cdot}$ and $(i\text{-}Pr_2S)_2^{+\cdot}$, was trapped in the ICR cell for more than 180 s, and no fragmentation was observed. The dissociation of $(i\text{-}Pr_2S)_2^{+\cdot}$ was found to be very slow, and therefore it was possible to study the equilibrium between $(i\text{-}Pr_2S)_2^{+\cdot}$ and three different dialkyl sulfide dimer radical cations, namely, $(MeEtS)_2^{+\cdot}$, $(Et_2S)_2^{+\cdot}$ and $(n\text{-}Bu_2S)_2^{+\cdot}$, vide infra.

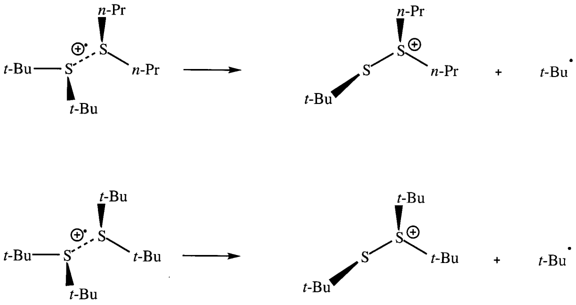

Scheme 1. Dissociation channels of the $(t\text{-}Bu_2S)_2^{+\cdot}$ and $(t\text{-}Bu_2S)(i\text{-}Pr_2S)^{+\cdot}$ dimer radical cations.

The radical cation of di-*t*-butyl sulfide was allowed to react in an environment of both *n*-Pr_2S and *t*-Bu_2S. Product ions appeared very rapidly and were identified as $(n\text{-}Pr_2S)_2^{+\cdot}$, $(n\text{-}Pr_2S)\ (t\text{-}Bu_2S)^{+\cdot}$, $(t\text{-}Bu_3S_2)^+$, $(n\text{-}Pr_2\text{-}t\text{-}BuS_2)^+$, and $(t\text{-}Bu_2S)_2^{+\cdot}$. Unfortunately, the abundance of the *t*-butyl sulfide dimer radical cations, $(t\text{-}Bu_2S)_2^{+\cdot}$ was too low for further study. It is obvious that the *t*-butyl groups have a large repulsive effect on the 2c3e S–S bond. Consequently, the $(t\text{-}Bu_2S)_2^{+\cdot}$ will eliminate a *t*-butyl group rapidly and produce the $(t\text{-}Bu_3S_2)^+$ ions, see Scheme I. Similarly, the mixed dimer radical cation, $(n\text{-}Pr_2S)\ (t\text{-}Bu_2S)^{+\cdot}$, fragments into $(n\text{-}Pr_2\text{-}t\text{-}BuS_2)^+$ and a *t*-butyl radical (Scheme 1).

The methanethiol dimer radical cation, $(CH_3SH)_2^{+\cdot}$, has also been generated using the association of the methanethiol radical cation with methanethiol. However, the product abundance of the dimer radical cations is found to be very low due to side reactions leading to product ions with molecular formula $(\text{dimer} - H)^+$ and $(\text{dimer} - H_2)^{+\cdot}$. Attempts to select the methanethiol dimer radical cation, with m/z 96, in the FT-ICR cell have failed, because the product ions with a mass corresponding to the ions with molecular formula $(\text{dimer} - H_2)^{+\cdot}$ and $(\text{dimer} - H)^+$ also have an isotopic abundance at m/z 96, namely the ^{34}S isotope of the $(\text{dimer} - H_2)^{+\cdot}$ ion, and both the ^{13}C isotope and the ^{33}S isotope of the $(\text{dimer} - H)^+$ ion.

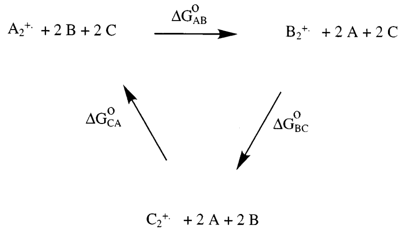

Scheme 2. Equilibrium triangle representing three equilibria; see further text.

3.2. Ligand exchange equilibrium measurements: Determination of ΔG^0

The studied dialkyl sulfide dimer radical cations have been found to react by ligand exchange with dialkyl sulfide molecules. This has allowed for the performance of equilibrium experiments between the dimer radical cations: $(Me_2S)_2^{+\cdot}$, $(MeEtS)_2^{+\cdot}$, $(Et_2S)_2^{+\cdot}$, $(Et\text{-}n\text{-}PrS)_2^{+\cdot}$, $(n\text{-}Pr_2S)_2^{+\cdot}$, $(i\text{-}Pr_2S)_2^{+\cdot}$, and $(n\text{-}Bu_2S)_2^{+\cdot}$. In general, a dialkyl sulfide dimer radical cation ($A_2^{+\cdot}$) undergoes a ligand exchange reaction with a dialkyl sulfide (B) producing the mixed dimer radical cation $AB^{+\cdot}$ [reaction (6)]. Subsequently, a second ligand exchange reaction produces the dimer radical cations of B [reaction (7)]:

$$A_2^{+\cdot} + B \rightarrow A + AB^{+\cdot} \tag{6}$$

$$AB^{+\cdot} + B \rightarrow A + B_2^{+\cdot} \tag{7}$$

Experimentally, an equilibrium is established between the radical cation dimers $A_2^{+\cdot}$, $AB^{+\cdot}$, and $B_2^{+\cdot}$ after a reaction time of approximately 10 s. The overall equilibrium constant, Eq. (4), i.e. for the equilibrium between $A_2^{+\cdot}$ and $B_2^{+\cdot}$, has been determined and from this the overall equilibrium Gibbs free energy difference ΔG^0_{AB} has been calculated using Eq. (5). To compare the different equilibria with each other, an equilibrium triangle has been drawn up, representing three dependent equilibria, see Scheme 2.

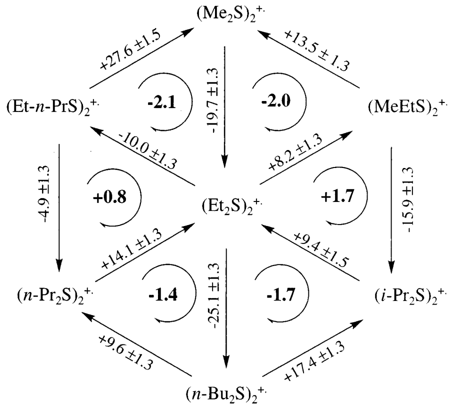

Scheme 3. Equilibrium studies between dialkyl sulfide dimer radical cations. Above each arrow the free energy difference (kJ mol^{-1}) is given. In the center of each triangle the sum of the free energies is given, which should be (close) to zero.

For each equilibrium triangle three ΔG^0 values have been determined independently. The ΔG^0_{AB} has been determined from the equilibrium between $A_2^{+\cdot}$ and $B_2^{+\cdot}$, the ΔG^0_{BC} has been determined from the equilibrium between $B_2^{+\cdot}$ and $C_2^{+\cdot}$ and the ΔG^0_{CA} has been determined from the equilibrium between $C_2^{+\cdot}$ and $A_2^{+\cdot}$. The Zeroth Law of Thermodynamics [18] states that if two substances *P* and *Q* are in equilibrium and in addition *Q* is in equilibrium with *R* then substances *P* and *R* are also in equilibrium. This means that in the equilibrium triangle depicted in Scheme 2, the Gibbs free energy is a conserved quantity and the surface integral of this equilibrium triangle must be zero:

$$\oint dG^0 = \Delta G^0_{AB} + \Delta G^0_{BC} + \Delta G^0_{CA} = 0 \tag{8}$$

We have checked to determine if our ΔG^0 values satisfy this condition within the experimental error given by the standard deviation of the ion product abundance ratio plus an error of 20% of the pressure readings of the compounds. Scheme 3 shows the results for six equilibrium triangles involving $(Me_2S)_2^{+\cdot}$, $(MeEtS)_2^{+\cdot}$, $(Et_2S)_2^{+\cdot}$, $(Et\text{-}n\text{-}PrS)_2^{+\cdot}$, $(n\text{-}Pr_2S)_2^{+\cdot}$, $(i\text{-}Pr_2S)_2^{+\cdot}$, and $(n\text{-}Bu_2S)_2^{+\cdot}$ (for simplicity, neutrals are not shown). Indeed, the surface integrals are, within the indicated error bars, nearly zero. Only one arrow of each equilibrium is drawn in Scheme 3, in order to indicate the direction of ΔG^0 in the calculations.

In Table 1, the obtained ΔG^0 values for the individual reactions (6) and (7) have been summarized. In addition, the ΔG^0 for the overall reaction has been written in Table 1.

Table 1
The Gibbs free energy change for the equilibria between the dialkyl sulfides ($A_2^{+\cdot}$ and $B_2^{+\cdot}$) and the mixed dimer radical cation ($AB^{+\cdot}$)

Compound		ΔG_1^{0} [a]	ΔG_2^{0} [b]	ΔG_{AB}^{0}
A	B	(kJ mol^{-1})	(kJ mol^{-1})	(kJ mol^{-1})
Me_2S	MeEtS	−7.5	−5.9	−13.5
Me_2S	Et_2S	−12.0	−7.6	−19.7
Me_2S	Et-*n*-PrS	−16.8	−10.6	−27.6
MeEtS	Et_2S	−6.0	−2.2	−8.2
MeEtS	*i*-Pr_2S	−12.0	−3.8	−15.9
Et_2S	Et-*n*-PrS	−6.5	−3.4	−10.0
Et_2S	*n*-Pr_2S	−8.1	−5.9	−14.1
Et_2S	*i*-Pr_2S	−6.2	−3.1	−9.4
Et_2S	*n*-Bu_2S	−14.4	−10.6	−25.1
Et-*n*-PrS	*n*-Pr_2S	−4.2	−0.7	−4.9
n-Pr_2S	*n*-Bu_2S	−6.5	−3.0	−9.6
i-Pr_2S	*n*-Bu_2S	−11.0	−6.3	−17.4

[a] For reaction: $A_2^{+\cdot} + B \rightarrow A + AB_2^{+\cdot}$.
[b] For reaction: $AB^{+\cdot} + B \rightarrow A + B_2^{+\cdot}$.

The Gibbs energy differences ΔG^0 thus obtained can be converted into enthalpy differences ΔH^0 and, eventually, into S–S bond dissociation enthalpies (BDE) using relationship (9):

$$\Delta G^0 = \Delta H^0 - T\Delta S^0 \tag{9}$$

The bond dissociation enthalpy (BDE) of a dimer radical cation is defined as the fragmentation enthalpy of dimer $A_2^{+\cdot}$ into a monomer radical cation and a monomer, Eqs. (10) and (11):

$$A + A^{+\cdot} \rightarrow A_2^{+\cdot} \tag{10}$$

$$\mathrm{BDE} = \Delta H_f^0[A_2^{+\cdot}] - \Delta H_f^0[A] - \Delta H_f^0[A^{+\cdot}] \tag{11}$$

Substitution of Eq. (11) into Eq. (9) yields Eq. (12) for equilibrium 3:

$$\begin{aligned}\Delta G_{AB}^0 = {} & \mathrm{BDE}(B_2^{+\cdot}) - \mathrm{BDE}(A_2^{+\cdot}) + \Delta H_f^0[B^{+\cdot}] \\ & - \Delta H_f^0[B] - \Delta H_f^0[A^{+\cdot}] \\ & + \Delta H_f^0[A] - T\Delta S^0\end{aligned} \tag{12}$$

The adiabatic ionization energy (IE) is defined as the difference between the enthalpy of formation of a radical cation and a neutral. This means that the Gibbs energy difference [Eq. (12)] is equal to the BDE difference of the dimer radical cations plus the difference of the ionization energy between B and A minus the entropy difference times the temperature, Eq. (13):

$$\begin{aligned}\Delta G_{AB}^0 = {} & \mathrm{BDE}(B_2^{+\cdot}) - \mathrm{BDE}(A_2^{+\cdot}) \\ & + [IE(B) - IE(A)] - T\Delta S^0\end{aligned} \tag{13}$$

The ionization energies of the compounds used in the present study are known [11,19] and summarized in Table 2. In addition, this table contains our experimentally determined Gibbs free energy difference ΔG^0 of each dimer radical cation relative to the radical cation dimer of diethyl sulfide.

In Fig. 1 the ionization energies of the dialkyl sulfides have been plotted versus the number of atoms. Fig. 1 shows that the IE decreases with increasing alkyl substituents. Di-*i*-propylsulfide has branched alkyl groups, and therefore this might be a reason why this compound does not fit the trend. Since the ionization energy of the ethyl-*n*-propylsulfide is reported to be larger than that of the smaller diethyl sulfide, it might be that the reported value refers to the vertical IE and not the adiabatic one. If the adiabatic ionization energy of the ethyl-*n*-propyl sulfide would follow the trend in Fig. 1, it will be around 8.35 eV, yielding $\Delta G^0 - \Delta\mathrm{IE} = 2.3$ kJ mol^{-1} for the equilibrium between ethyl-*n*-propylsulfide and diethyl sulfide.

Table 2
Sulfur–sulfur bond dissociation energies (BDE) of $(R_2S)_2^{+\cdot}$ dimer radical cations derived from experimental Gibbs free energy changes (experiment) and theoretical entropy changes for the equilibrium given in Eq. (14). In addition, this table summarizes the ionization energies and bond dissociation energies from the literature

Compound (Y)	ΔG^0 [a] (kJ mol^{-1})	$\Delta S^0_{\text{total}}$ [a] (J mol^{-1} K^{-1})	IE [b] (eV)	$\Delta G^0 - \Delta$IE (kJ mol^{-1})	BDE [a] (kJ mol^{-1})	BDE [c] (kJ mol^{-1})
Me_2S	−19.7	−17.9 [d]	8.69 ± 0.01	5.4	115	111 [j]
MeEtS	−8.2	3.9 [d]	8.54 ± 0.01	2.4	112	
Et_2S	0.0	0.0 [d]	8.43 ± 0.01	0.0	115	115 [j,k]
Et-*n*-PrS	10.0	18.7 [e]	8.50 ± 0.05	2.3 [h]	107 [h]	
n-Pr_2S	14.1	36 [f]	8.30 ± 0.02	1.6	103	97 [k],119 [f]
n-Bu_2S	25.1	50 [g]	8.20 ± 0.10	2.9	97	89 [k]
i-Pr_2S	9.4	25 [g]	8.00 ± 0.10	−32.1	140 [i]	

[a] This work.
[b] Values from Lias et al. [11,19].
[c] Literature values.
[d] Calculated at the HF/6-31G(*d*) level of theory; the vibrational entropy change has been neglected.
[e] Calculated at the HF/3-21G level of theory; the vibrational entropy change has been neglected.
[f] [6].
[g] Estimated from Fig. 3.
[h] An ionization energy of 8.35 eV has been used in this calculation, see text for explanation.
[i] Due to a large uncertainty in the IE (see Fig. 1) this BDE does not follow the trend.
[j] [4].
[k] [7].

If the entropic contributions $T\Delta S^0$ were negligible then, according to Eq. (13), the Gibbs free energy difference minus the difference in ionization energies between B and A would give the BDE difference between the two dimer radical cations. However, it is anticipated that the difference $\Delta G^0 - \Delta\text{IE}$ of ~0–5 kJ mol^{-1} [for $(i\text{-}Pr_2S)_2^{+\cdot}$ it is larger, see Table 2] is of the same order as the entropy contribution $T\Delta S^0$. Therefore, in the next section the contributions of the entropy to the studied equilibria will be discussed.

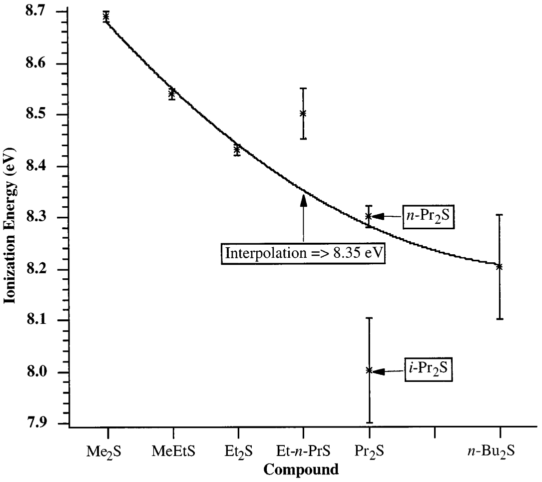

Fig. 1. The ionization energies (IE) of the dialkyl sulfides as a function of the number of atoms per molecule. The line has been added to guide the eye.

3.2. Estimation of entropies using statistical thermodynamics

The experimental determination of the entropic contributions to the Gibbs free energy changes of the studied equilibria requires variation of the temperature. In the FT-ICR mass spectrometer used this is not possible. The entropy contributions, therefore, have been estimated using statistical thermodynamics [18,20].

3.2.1. Translational entropy

Because in Table 2 the ΔG^0 are given relative to the diethyl sulfide dimer radical cation, the entropic

Table 3
The translational entropy for equilibrium 14, calculated with Eq. (15)

Compound (Y)	ΔS^0_{tr} (J mol^{-1} K^{-1})	$T\ \Delta S^0_{\mathrm{tr}}$ [a] (kJ mol^{-1})
$\mathrm{Me_2S}$	−4.65	−1.39
MeEtS	−2.11	−0.63
$\mathrm{Et_2S}$	0.00	0.00
Et-*n*-PrS	1.81	0.54
n-$\mathrm{Pr_2S}$	3.38	1.00
i-$\mathrm{Pr_2S}$	3.38	1.00
n-$\mathrm{Bu_2S}$	6.04	1.80

[a] The temperature has been assumed to be 298 K.

contribution has been calculated for the same reactions, Eq. (14):

$$\mathrm{Y_2^{+\cdot}} + 2\mathrm{Et_2S} \rightarrow 2\mathrm{Y} + (\mathrm{Et_2S})_2^{+\cdot} \tag{14}$$

The corresponding translational entropy of reaction depends only on the ratio of m_{Y} and $m_{\mathrm{Et_2S}}$ as can be seen in Eq. (15). Table 3 lists the ΔS^0_{tr} for all compounds studied, calculated with Eq. (15):

$$\Delta S^0_{\mathrm{tr}} = \frac{3}{2} R \ln\left(\frac{m^2_{\mathrm{Y}}}{m^2_{\mathrm{Et_2S}}} \frac{m_{(\mathrm{Et_2S})_2^{+\cdot}}}{m_{\mathrm{Y}_2^{+\cdot}}}\right) = \frac{3}{2} R \ln \frac{m_{\mathrm{Y}}}{m_{\mathrm{Et_2S}}} \tag{15}$$

3.2.2. Rotational entropy

Eq. (16) shows how the rotational entropy change $\Delta S^0_{\mathrm{rot}}$ associated with equilibrium 14 depends on the principal moments of inertia (A, B, C) and symmetry numbers (σ) and, therefore, on the structure of the various adducts and products:

$$\Delta S^0_{\mathrm{rot}} = \frac{1}{2} R \ln\left(\frac{\mathrm{A^2B^2C^2}_{\mathrm{Y}}}{\mathrm{ABC}_{\mathrm{Y}_2^{+\cdot}}} \frac{\mathrm{ABC}_{(\mathrm{Et_2S})_2^{+\cdot}}}{\mathrm{A^2B^2C^2_{Et_2S}}}\right) + R \ln\left(\frac{\sigma_{\mathrm{Y}_2^{+\cdot}}}{\sigma^2_{\mathrm{Y}}} \frac{\sigma^2_{\mathrm{Et_2S}}}{\sigma_{(\mathrm{Et_2S})_2^{+\cdot}}}\right) \tag{16}$$

The structures of the ions and molecules have been predicted computationally. Some of our larger systems are computationally difficult or not accessible with ab initio methods. Therefore, we have examined the suitability of a semi-empirical AM1 approach for geometry optimization and computation of rotational entropies. This was done by comparing AM1 and MP2/6-31G(*d*) results for $\mathrm{Me_2S}$ and $\mathrm{Et_2S}$ (Table 4).

Table 4
Bond distances (Å), bond angles (degrees), and rotational entropy (J mol^{-1} K^{-1}) of $\mathrm{Me_2S}$ and $\mathrm{Et_2S}$

	$\mathrm{Me_2S}$		$\mathrm{Et_2S}$	
	AM1	MP2/6-31G(*d*)	AM1	MP2/6-31G(*d*)
Bond distances				
r(S–C1)	1.752	1.807	1.770	1.815
r(C1–H)	1.113	1.093	1.117	1.095
r(C1–C2)	· · ·	· · ·	1.500	1.524
r(C2–H)	· · ·	· · ·	1.118	1.093
Bond angles				
a(C1–S–C1)	102.8	98.6	101.7	99.1
a(S–C1–H)	112.0	111.3	110.0	109.2
a(S–C1–C2)	· · ·	· · ·	107.8	110.0
a(C1–C2–H)	· · ·	· · ·	110.8	111.0
Rotational entropy				
S^0_{rot}	92.3	98.5	104.7	105.1

AM1 optimized geometry parameters differ by some 5% from the MP2/6-31G(*d*) values. In particular, the S–C bond distances are reduced, whereas the C–S–C angles increase. The former effect tends to make the molecules more compact and to reduce their moments of inertia. This is counteracted by the increase in *a*(C1–S–C1). Therefore, the moments of inertia and thus the rotational entropies $\Delta S^0_{\mathrm{rot}}$ [Eq. (15)] have similar values at AM1 and MP2: for dimethyl sulfide the AM1 value of $\Delta S^0_{\mathrm{rot}}$ is 6% smaller than the MP2 one; for diethyl sulfide the agreement is even excellent, $\Delta S^0_{\mathrm{rot}}$ being only 0.4% smaller at AM1 than at MP2. These deviations are much smaller than the uncertainty associated with the experimental data used (e.g. IE, ΔG^0, ΔH^0_f). We therefore conclude that the AM1 results are sufficiently accurate for our purpose.

The rotational entropy of $\mathrm{Et_2S^{+\cdot}}$ is 105.0 J mol^{-1} K^{-1} at UMP2/6-31G(*d*,*p*) (Table 5). This value is quite robust with respect to changes in the theoretical level: at ROHF/3-21G $\Delta S^0_{\mathrm{rot}}$ is still 105.9 kcal/mol, only 1% larger than at UMP2/6-31G(*d*,*p*). The LDA value of 97.9 J mol^{-1} K^{-1} is 7% smaller.

The dimer radical cations $(\mathrm{Me_2S})_2^{+\cdot}$ and $(\mathrm{Et_2S})_2^{+\cdot}$, too, were computationally examined using AM1 as well as ab initio theory at MP2/6-31G(*d*) and HF/6-

Table 5
The rotational entropy as a function of the basis set for $Et_2S^{+\cdot}$

Level of theory	Basis set	S^0_{rot} (J mol^{-1} K^{-1})
ROHF	3-21G	105.90
ROHF	4-31G(*d*)	105.88
ROHF	6-31G(*d*,*p*)	105.82
UHF	6-31G(*d*)	105.12
UHF	6-31G(*d*,*p*)	105.11
UMP2	6-31G(*d*)	105.00
UMP2	6-31G(*d*,*p*)	104.98

31G(*d*), respectively. Selected geometry parameters and the rotational entropies are summarized in Table 4. The AM1 and ab initio structures differ significantly and, as far as the length of the S–S 2c3e bond is concerned, even dramatically. In $(Me_2S)_2^{+\cdot}$, for instance, *r*(S–S) is 2.795 Å at MP2/6-31G(*d*). This agrees reasonably with preliminary DFT results of 2.753 (LDA) and 2.911 Å (BP86). But at AM1, *r*(S–S) is only 2.278 Å, i.e. more than 0.5 Å or 18% shorter than at MP2! Similarly, the S–S bond in $(Et_2S)_2^{+\cdot}$ contracts by 0.6 Å (21%) on going from HF/6-31G(*d*) to AM1. Yet, the difference of 3%–8% between AM1 and ab initio rotational entropies ΔS^0_{rot} is relatively modest, because again the effect of the reduced *r*(S–S) on the moments of inertia is counteracted, amongst others, by that of the increased *a*(S–S–C1). For example, ΔS^0_{rot} of $(Me_2S)_2^{+\cdot}$ is 112.7 and 114.1 J K^{-1} mol^{-1} at AM1 and MP2 (Table 6). The LDA value of 119.2 J K^{-1} mol^{-1} is somewhat larger. Furthermore, for $(Et_2S)_2^{+\cdot}$ two distinct equilibrium structures, with C_2 and C_{2h} point group symmetry, respectively, were found at HF/6-31G(*d*) (see Fig. 2). The corresponding rotational entropies of 125.6 J mol^{-1} K^{-1} (C_2) and 125.8 J mol^{-1} K^{-1} (C_{2h}), however, differ only marginally.

The overall rotational entropy for equilibrium (14) with $Y = Me_2S$ is -18.0 J mol^{-1} K^{-1} at the AM1 level, while a value of -17.9 J mol^{-1} K^{-1} at the HF/6-31G(*d*) level of theory has been obtained. Notwithstanding the large geometry differences, these rotational entropies imply that the AM1 level of theory is a good alternative for rotational entropy calculations.

Table 6
Bond distances (Å) and bond angles (degrees) of $(Me_2S)_2^{+\cdot}$ and $(Et_2S)_2^{+\cdot}$ both in the C_{2H} symmetry

	$(Me_2S)_2^{+\cdot}$		$(Et_2S)_2^{+\cdot}$	
	AM1	MP2/6-31G(*d*)	AM1	HF/6-31G(*d*)
Bond distances				
r(S–S)	2.278	2.795	2.277	2.875
r(S–C1)	1.755	1.804	1.786	1.828
r(C1–H)	1.117	1.092	1.120	1.082
r(C1–C2)	· · ·	· · ·	1.499	1.526
r(C2–H)	· · ·	· · ·	1.120	1.083
Bond angles				
a(S–S–C1)	104.5	95.6	101.9	98.6
a(C1–S–C1)	102.9	100.6	103.0	102.5
a(S–C1–H)	109.9	110.8	108.6	108.6
a(S–C1–C2)	· · ·	· · ·	108.4	111.0
a(C1–C2–H)	· · ·	· · ·	110.8	111.2
Rotational entropy				
S^0_{rot}	112.7	114.1	124.2	125.8

3.2.3. Vibrational entropy

The vibrational entropy is given by Eq. (17). Here, *R* is the gas constant, *h* Planck's constant, *k* Boltzmann's constant, *T* the absolute temperature, and ν the vibrational frequency:

$$S^0_{vib} = \sum_{\nu} - R \ln\left[1 - \exp\left(-\frac{h\nu}{kT}\right)\right] + R\left(\frac{h\nu}{kT}\right) \times [\exp(-h\nu/kT)/1 - \exp(-h\nu/kT)] \qquad (17)$$

Vibrational frequencies are typically between 0 and 3500 cm^{-1}. The entropy is mainly determined by the lower frequencies, because the low-frequency oscillators provide the largest contributions to the partition function [18,20].

In order to study the order of magnitude of the vibrational entropy change for the studied equilibria, the calculated entropy change has been compared to experimentally determined values of Deng et al. [4]. They have experimentally studied the equilibrium between the dimethyl sulfide dimer radical cation and its ionized and neutral monomers [Eq. (18)]. They also measured such an equilibrium for the diethyl sulfide system [Eq. (19)]. By analyzing the effect of changing the temperature and with the help of van 't Hoff plots, Deng et al. determined both the enthalpy and entropy of reaction:

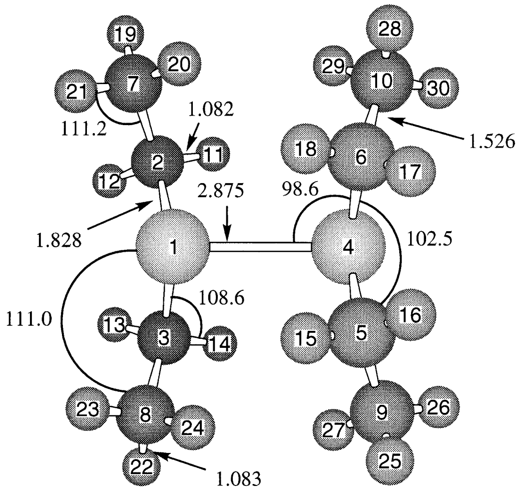

A $(Et_2S)_2^{+\cdot}$ in the C_{2H} symmetry

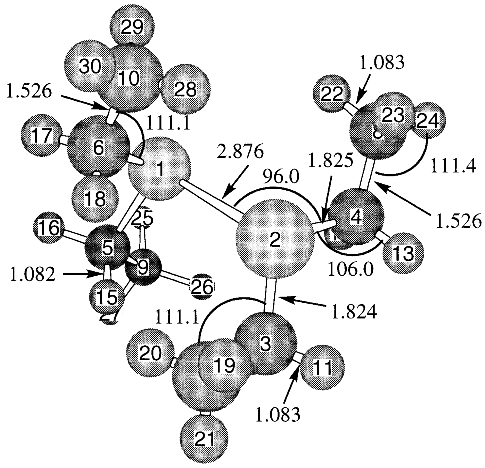

B $(Et_2S)_2^{+\cdot}$ in the C_2 symmetry

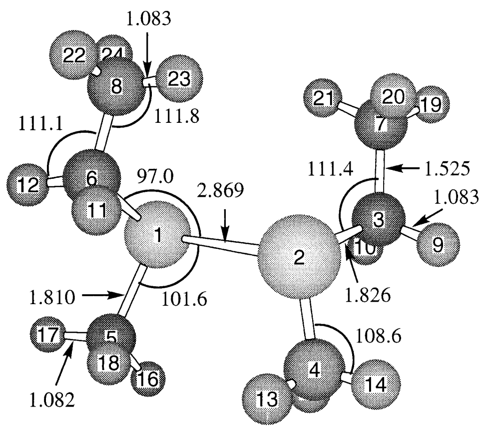

C $(MeEtS)_2^{+\cdot}$ in the C_2 symmetry

Table 7

The translational, rotational, and vibrational entropy for the species of Eq. (20) calculated at the HF/6-31G(*d*) level of theory. In addition, for each type of entropy the sum (products minus reactants) has been added

Compound [a]	S^0_{trans} (J mol^{-1} K^{-1})	S^0_{rot} (J mol^{-1} K^{-1})	S^0_{vib} (J mol^{-1} K^{-1})
Reactants			
$(Me_2S)_2^{+\cdot}$	168.8	114.4	143.9
$Et_2S^{+\cdot}$	164.9	105.0	84.4
Et_2S	164.9	105.0	72.6
Products			
$Me_2S^{+\cdot}$	160.2	92.7	36.0
Me_2S	160.2	92.8	27.3
$(Et_2S)_2^{+\cdot}$	173.5	125.6	241.2
Total	−4.7	−13.3	+3.6 [b]

[a] Ionized and neutral monomers in the C_{2V} symmetry, $(Me_2S)_2^{+\cdot}$ in the C_{2H} symmetry and $(Et_2S)_2^{+\cdot}$ in the C_2 symmetry.

[b] Unscaled; using scaled frequencies $\Delta S^0_{\text{vib}} = +3.7$ J mol^{-1} K^{-1}.

$$(Me_2S)_2^{+\cdot} + Q \rightleftarrows Me_2S^{+\cdot} + Me_2S + Q \tag{18}$$

$$(Et_2S)_2^{+\cdot} + Q \rightleftarrows Et_2S^{+\cdot} + Et_2S + Q \tag{19}$$

Adding Eqs. (18) and (19), we obtain the double ligand exchange equilibrium of Eq. (20). To estimate the entropy change associated with this equilibrium reaction, we have performed ab initio calculations at the HF/6-31G(*d*) level.

$$(Me_2S)_2^{+\cdot} + Et_2S^{+\cdot} + Et_2S \rightleftarrows Me_2S^{+\cdot} + Me_2S + (Et_2S)_2^{+\cdot} \tag{20}$$

Table 7 displays the translational, rotational, and vibrational entropies of the species in Eq. (20). The sum of the translational entropy and the rotational entropy change is −17.9 J mol^{-1} K^{-1} (at 298 K). This is in good agreement with the experimental result [4] of −20 J mol^{-1} K^{-1}, which is based on measurements of equilibrium 18 (at 576 K) and equilibrium (19) (at 520 K). The vibrational entropy change is positive, due to several low frequencies. Ignoring all frequencies below 300 cm^{-1} gives a vibrational entropy change of −0.2 J mol^{-1} K^{-1} and then will

Fig. 2 (*see left column*). Optimized geometries (HF/6-31G(*d*) level of theory) of $(Et_2S)_2^{+\cdot}$, C_{2H} symmetry. (a) and C_2 symmetry, (b) and $(MeEtS)_2^{+\cdot}$, (c) dimer radical cations. Bond distances are in Å and bond angles in degrees.

become negligible. In conclusion, the sum of the translational and rotational entropy at the HF/6-31G(*d*) or AM1 level of theory gives a good estimation of the entropy of reaction 14. Therefore, in the case of the equilibrium between the dimer radical cations of methylethyl sulfide and diethyl sulfide the entropy has been calculated at the HF/6-31G(*d*) level of theory.

3.3. Sulfur–sulfur bond dissociation energies

In Table 2, we summarize our experimental ΔG^0 values for equilibrium 14, together with the corresponding ΔS^0 values. For the smaller species, i.e. $(Me_2S)_2^{+\cdot}$, $(MeEtS)_2^{+\cdot}$, and $(Et_2S)_2^{+\cdot}$, these ΔS^0 values stem from our HF/6-31G(*d*) computations. As has been shown above the ΔS^0 for the equilibrium is mainly dependent on the rotational and translational part of the entropy. Moreover, low level calculations have been shown to give results which are in good agreement with higher level calculations. Therefore, the equilibrium that involves the $(Et\text{-}n\text{-}PrS)_2^{+\cdot}$ dimer radical cation has been calculated at the HF/3-21G level of theory. The remaining ΔS^0 values for the larger $(n\text{-}Pr_2S)_2^{+\cdot}$, $(i\text{-}Pr_2S)_2^{+\cdot}$, and $(n\text{-}Bu_2S)_2^{+\cdot}$ systems, were either estimated or collected values from the literature.

Two different $(MeEtS)_2^{+\cdot}$ dimer radical cations have been considered in the calculations, one with C_2 symmetry and one with C_i symmetry. The species with C_2 symmetry has been found to be a minimum energy structure, see Fig. 2. Ionized and neutral methyl ethyl sulfide monomers have been calculated with C_S symmetry.

Recently, James and Illies [6] have determined the association entropy of $(n\text{-}Pr_2S)_2^{+\cdot}$. Using van 't Hoff plots they determined ΔH^0 and ΔS^0 of reaction (21):

$$(n\text{-}Pr_2S)_2^{+\cdot} + Q \rightleftarrows n\text{-}Pr_2S^{+\cdot} + n\text{-}Pr_2S + Q \qquad (21)$$

Together with the experimental entropies obtained by Deng et al. [4] for Eqs. (18) and (19), these data enable us to compute the entropy change $\Delta S^0 = 36$ J mol^{-1} K^{-1} associated with equilibrium (22) (see Table 2):

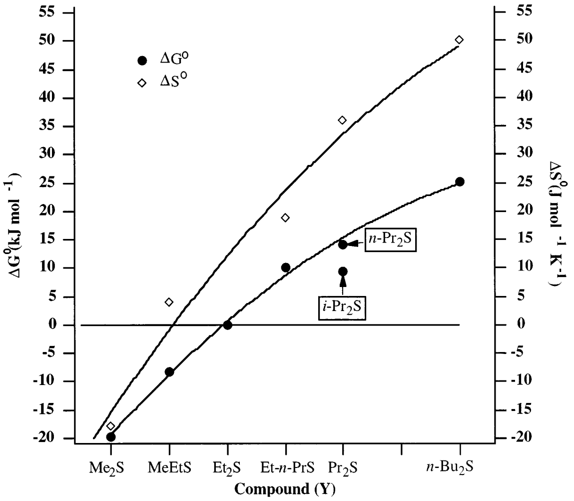

Fig. 3. The Gibbs free energy change (ΔG^0, this work) and the entropy difference (ΔS^0) of dialkyl sulfide dimer radical cations plotted versus the number of atoms. For an explanation see the text.

$$(n\text{-}Pr_2S)_2^{+\cdot} + Et_2S^{+\cdot} + Et_2S \rightleftarrows n\text{-}Pr_2S^{+\cdot} + n\text{-}Pr_2S + (Et_2S)_2^{+\cdot} \qquad (22)$$

Our experimental Gibbs free energies and the calculated or estimated entropies for the equilibria mentioned above are visualized in Fig. 3 as a function of the number of atoms. The reaction entropies for the equilibrium exchange reactions 14 with $Y = n\text{-}Bu_2S$ and $i\text{-}Pr_2S$ have been estimated from these data through interpolation (see Table 2).

Finally, the sulfur–sulfur bond dissociation enthalpy can be computed using Eq. (13), the data in Table 2, and the literature [4,7] value of 115 kJ mol^{-1} for the BDE of $(Et_2S)_2^{+\cdot}$. The resulting BDE are also collected in Table 2. The overall trend, going from small to large $(R_2S)_2^{+\cdot}$ dimers, is a decrease in the S–S bond strength from 115 kJ mol^{-1} for $(Me_2S)_2^{+\cdot}$ to 97 kJ mol^{-1} for $(n\text{-}Bu_2S)_2^{+\cdot}$. An exception on this trend is the "too high" S–S BDE of 140 kJ mol^{-1} for $(i\text{-}Pr_2S)_2^{+\cdot}$.

The presently determined BDE values agree well with those from literature. For example, Deng et al. [4] have calculated bond dissociation enthalpies of 118.4 kJ mol^{-1} for $(Me_2S)_2^{+\cdot}$ and 117.0 kJ mol^{-1} for $(Et_2S)_2^{+\cdot}$ at the MP2/6-31G(*d*) level; their corresponding experimental values are 111 ± 2 and 116 ± 3 kJ mol^{-1}, respectively. This is close to our 115 kJ mol^{-1}. Surprisingly, the calculated energies at the HF/6-31G(d) level of theory lead to a drop in the BDE to 60.4 kJ mol^{-1} for $(Me_2S)_2^{+\cdot}$, almost half the BDE calculated at the MP2/6-31G(d) level! Furthermore, there is a good agreement with the results from our recent threshold experiments [7]. The latter have yielded bond dissociation energies of 115 ± 10, 98 ± 10, and 89 ± 10 kJ mol^{-1} for $(Et_2S)_2^{+\cdot}$, $(n\text{-}Pr_2S)_2^{+\cdot}$, and $(n\text{-}Bu_2S)_2^{+\cdot}$, which has to be compared with the 115, 103, and 97 kJ mol^{-1}, respectively, obtained from the present equilibrium experiments.

Possible electronic effects on the S–S bond strength [21] are expected to be most pronounced for the smaller dimers, e.g. when going from $(Me_2S)_2^{+\cdot}$ to $(Et_2S)_2^{+\cdot}$ or, even more so, from $(H_2S)_2^{+\cdot}$ to $(Me_2S)_2^{+\cdot}$, because here the characteristics of the $R^{\cdot}$ sustituent's electronic structure, such as the polarizability or the energy of the singly occupied molecular orbital (SOMO), relatively change the most. Yet, and this is of particular interest, the S–S bond strength is more or less constant along $(Me_2S)_2^{+\cdot}$, $(MeEtS)_2^{+\cdot}$, and $(Et_2S)_2^{+\cdot}$. Only when propyl or larger substituents R are introduced, the BDE begins to decrease more significantly. This strongly suggests that it is steric repulsion between alkyl groups across the S ∴ S bond that begins to oppose the 2c3e bonding interactions. In line with this is the low stability of $(n\text{-}Pr_2S)(t\text{-}Bu_2S)^{+\cdot}$ and $(t\text{-}Bu_2S)_2^{+\cdot}$ both of which rapidly eliminate a t-butyl group. The rather late onset of the repulsive forces may be ascribed to the fact that the S ∴ S 2c3e bond is relatively long with ~2.9 Å (for comparison, the S–S single bond in CH_3SSCH_3 is with ~2.0 Å much shorter) [21].

4. Conclusions

We have determined the S–S bond dissociation energies (BDE) of a series of dialkyl sulfide dimer radical cations using FT-ICR mass spectrometry. The smaller dimers $(Me_2S)_2^{+\cdot}$, $(MeEtS)_2^{+\cdot}$, and $(Et_2S)_2^{+\cdot}$ all have comparable S–S bond strengths with a BDE of approximately 115 kJ mol^{-1}. The larger dimers show a steady decrease of the S–S bond dissociation energy with increasing size of the alkyl groups. This is ascribed to steric repulsion between alkyl groups across the S ∴ S bond. The rather late onset of the repulsive forces is ascribed to the fact that the S ∴ S 2c3e bond is relatively long with ~2.9 Å.

The ΔG^0s of the ligand exchange equilibria $(R_2S)_2^{+\cdot} + 2\ Et_2S \rightleftarrows (Et_2S)_2^{+\cdot} + 2\ R_2S$ have a significant entropy contribution $T\Delta S^0$ as appears from our computations at various levels of theory, ranging from semi-empirical to ab initio (used for the BDE values) and DFT. The entropy change ΔS^0 is shown to originate primarily from the change in rotational entropy ΔS^0_{rot}.

Supplementary material

Cartesian coordinates, energies and entropies of Me_2S, $Me_2S^{+\cdot}$, Et_2S, $Et_2S^{+\cdot}$ (all in C_{2v} symmetry), MeEtS, $MeEtS^{+\cdot}$, and Et-n-PrS (C_S symmetry), $(Me_2S)_2^{+\cdot}$ (C_{2h} symmetry), $(MeEtS)_2^{+\cdot}$ (C_2 symmetry), $(Et_2S)_2^{+\cdot}$ (C_2 and C_{2h} symmetry) and $(Et\text{-}n\text{-}PrS)_2^{+\cdot}$ (C_2 symmetry) are available upon request (8 pages).

Acknowledgements

The authors wish to thank the Netherlands Organization for Scientific Research (NWO/SON/NCF) for financial support. F.M.B. thanks the Deutsche Forschungsgemeinschaft (DFG) for a Habilitanden fellowship.

References

[1] T. Drewello, C.B. Lebrilla, H. Schwarz, L.J. de Koning, R.H. Fokkens, N.M.M. Nibbering, E. Anklam, K.-D. Asmus, J. Chem. Soc. Chem. Commun. (1987) 1381.
[2] A.J. Illies, P. Livant, M.L. McKee, J. Am. Chem. Soc. 110 (1988) 7980.
[3] S. Ekern, A.J. Illies, M.L. McKee, M.J. Peschke, J. Am. Chem. Soc. 115 (1993) 12510.
[4] Y. Deng, A.J. Illies, M.A. James, M.L. McKee, M.J. Peschke, J. Am. Chem. Soc. 117 (1995) 420.
[5] M.A. James, M.L. McKee, A.J. Illies, J. Am. Chem. Soc. 118 (1996) 7836.

[6] M.A. James, A.J. Illies, J. Phys. Chem. 100 (1996) 15794.

[7] S.P. de Visser, L.J. de Koning, N.M.M. Nibbering, Int. J. Mass Spectrom. Ion Processes 157 (1996) 283.

[8] P. Livant, A.J. Illies, J. Am. Chem. Soc. 113 (1991) 1510.

[9] (a) S.P. de Visser, L.J. de Koning, N.M.M. Nibbering, J. Am. Chem. Soc. 120 (1998) 1517. (b) L.S. Nichols, M.L. McKee, A.J. Illies, J. Am. Chem. Soc. 120 (1998) 1538.

[10] S.P. de Visser, L.J. de Koning, N.M.M. Nibbering, J. Phys. Chem. 99 (1995) 15444.

[11] S.G. Lias, J.E. Bartmess, J.F. Liebman, J.L. Holmes, R.D. Levin, W.G. Mallard, J. Phys. Chem. Ref. Data, Suppl. 1, 17 (1988).

[12] A.J.R. Heck, T. Drewello, L.J. de Koning, N.M.M. Nibbering, Int. J. Mass Spectrom. Ion Processes 100 (1990) 611.

[13] L.J. de Koning, R.H. Fokkens, F.A. Pinkse, N.M.M. Nibbering, Int. J. Mass Spectrom. Ion Processes 77 (1987) 95.

[14] J.E. Bartmess, R.M. Georgiadis, Vacuum 33 (1983) 149.

[15] K.J. Miller, J. Am. Chem. Soc. 112 (1990) 8533.

[16] M.J. Frisch, G.W. Trucks, H.B. Schlegel, P.M.W. Gill, B.G. Johnson, M.A. Robb, J.R. Cheeseman, T. Keith, G.A. Petersson, J.A. Montgomery, K. Raghavachari, M.A. Al-Laham, V.G. Zakrzewski, J.V. Ortiz, J.B. Foresman, J. Cioslowski, B.B. Stefanov, A. Nanayakkara, M. Challacombe, C.Y. Peng, P.Y. Ayala, W. Chen, M.W. Chong, J.L. Andres, E.S. Replogle, R. Gomperts, R.L. Martin, D.J. Fox, J.S. Binkley, D.J. Defrees, J. Baker, J.P. Stewart, M. Head-Gordon, C. Gonzalez, J.A. Pople, Gaussian, Inc., Pittsburgh, PA, 1995.

[17] (a) C. Fonseca Guerra, O. Visser, J.G. Snijders, G. te Velde, E.J. Baerends, in *METECC-95* (E. Clementi, and G. Corongiu Eds.), STEF, Cagliari, 1995, pp. 305–395; (b) G. te Velde, E.J. Baerends, J. Comp. Phys. 99 (1992) 84; (c) S.H. Vosko, L. Wilk, M. Nusair, Can. J. Phys. 58 (1980) 1200; (d) A.D. Becke, Phys. Rev. A 38 (1988) 3098; (e) J.P. Perdew, Phys. Rev. B 33 (1986) 8822; (f) F.M. Bickelhaupt, N.M.M. Nibbering, E.M. van Wezenbeek, E.J. Baerends, J. Phys. Chem. 96 (1992) 4864; (g) T. Ziegler, A. Rauk, Theoret. Chim. Acta 46 (1977) 1.

[18] P.W. Atkins, Physical Chemistry, 5th ed., Oxford University Press, Oxford, 1994.

[19] S.G. Lias, J.F. Liebman, R.D. Levin, S.A. Kafafi, N.I.S.T. Standard Reference Database 19A, Version 2-01 (1994).

[20] G.M. Barrow, Physical Chemistry, 6th ed., McGraw-Hill, New York, 1996.

[21] For a discussion of the bonding in RSSR see, for example, F.M. Bickelhaupt, M. Solà, P. v.R. Schleyer, J. Comput. Chem. 16 (1995) 465.